

ORIGINAL ARTICLE

Influence of Active Flow Control on Blunt-Edged VFE-2 Delta Wing model

I. Madan¹, N. Tajuddin¹, M. Said¹, S. Mat¹, N. Othman¹, M.A. Wahid¹, N.H. Mohamed Radzi¹, J.J. Miao², Y.R. Chen² and L.Y. Chen²

¹Faculty of Mechanical Engineering, Universiti Teknologi Malaysia, 81200 Skudai, Johor Bahru, Johor, Malaysia

²Department of Aeronautics and Astronautics, National Cheng Kung University, Tainan 7010, Taiwan

ABSTRACT – This paper highlights the flow topology above blunt-edged delta wing of VFE-2 configuration when an active flow control technique called ‘blower’ is applied in the leading edge of the wing. The flow topology above blunt-edged delta wing is very complex, disorganised and unresolved compared to sharp-edged wing. For the sharp leading-edged wing, the onset of the primary vortex is fixed at the apex of the wing and develops along the entire wing towards the trailing edge. However, the onset of the primary vortex is no longer fixed at the apex of the wing for the blunt-edged case. The onset of the primary vortex develops at a certain chord-wise position and it moved upstream or downstream depending on Reynolds number, angle of attack, Mach number and the leading-edge bluntness. An active flow control namely ‘blower’ technique has been applied in the leading edge of the wing in order to investigate the upstream/downstream progression of the primary vortex. This research has been carried out in order to determine either the flow on blunt-edged delta wing would behave as the flow above sharp-edged delta wing if any active flow control is applied. The experiments were performed at Reynolds number of 0.5×10^6 , 1.0×10^6 and 2.0×10^6 corresponding to 9 m/s, 18 m/s and 36 m/s in UTM Low Speed wind Tunnel based on the mean aerodynamic chord of the wing. The results obtained from this research have shown that the blower technique has significant effects on the flow topology above blunt-edged delta wing. The main observation from this study was that the primary vortex has been shifted 20% upstream when the blower technique is applied. Another main observation was the ability of this flow control to delay the formation of the vortex breakdown.

ARTICLE HISTORY

Received: 16th April 2020

Revised: 8th Oct 2020

Accepted: 16th Dec 2020

KEYWORDS

Delta wing, VFE-2;

Active flow control;

Primary vortex;

Wind tunnel experiment

INTRODUCTION

In the early 1980s, many researches have been performed to identify the ability of the Euler Method to calculate the vertical flow above the delta wing correctly. A research group calls the First International Vortex Flow Experiment (VFE-1) was established. The numerical calculation was performed on sharp-edged and blunt-edged in the period between 1984-1986. At that time, the Euler method codes were not suitable to calculate the pressure distribution for the sharp-edged delta wing because the secondary vortex cannot be modelled. The second International Vortex Flow Experiment (VFE-2) was then established within Research and Technology Organization (RTO) under the Applied Vehicle Technology (AVT) symposium in Leon 2001 to investigate further the capability of CFD codes to estimate the flow characteristics above the blunt-edged wing. For this group, the calculations were performed on both, sharp and blunt-edged wing. The data obtained from CFD calculations were then compared with the wind tunnel testing data [1]. The outcome from the VFE-2 was that the vortex flow characteristics are complicated for the blunt leading edge, where the onset of the primary vortex is no longer fixed at the apex of the wing. At the low to moderate angle of attack, the flow is attached to the wing surface. When the angle of attack is further increased, the flow separated near the wing tip due to the up-wash distribution at the delta wing leading edge. The formations of the primary vortex were affected by some factors such as leading-edge bluntness, Mach number, Reynolds number and angle of attack [2]. The current study has been carried out to verify the ability of the flow control technique to change the flow characteristics above the wing. There were several flow control techniques available, and one of them is called it the ‘blower’ technique. A recent study has shown that this technique can increase the magnitude of the primary vortex and the negative pressure coefficient at a higher angle of attack [16, 17, 18, 19, 20]. However, it is not certain whether the technique can move the onset of the primary vortex to the apex of the wing.

LITERATURE REVIEW

The flow topology above sharp-edged delta wing is dominated by a flow phenomenon called as a primary vortex. As the angle of attack is increased, the magnitude of this primary vortex increased. The primary separation line is fixed at the leading edge of the wing. Underneath the primary vortex, another vortex called as secondary vortex appears due to the strong side flow toward the leading edge [3]. The suction peak of the primary vortex takes a conical shape above the

wing, and its magnitude decreases downstream towards the trailing edge. At certain condition, turbulent secondary separation may take place outboard of the suction peak [3, 4].

The flow characteristic above the blunt-edge wing is rather complicated. The primary separation line is not fixed to the leading edge but somewhere in the region close to the leading edge. The attached non-separation flow occurred on the wing at a low angle of attack. The primary vortex developed further aft of the wing at certain chord wise position. The onset of the flow separation for rounded leading edge can be explained by the flow separation, takes place at a certain position downstream from the apex due to the small ratio between the wingspan and the leading-edge radius [6, 7]. The flow characteristics are much dependent on the angle of attack, Reynolds number, leading-edge radius and Mach number. For the angle of attack, the onset of flow separation and formation of the primary vortex strongly depend on the angle of attack. The primary vortex moved upstream to the apex region when the angle of attack increased. Several numerical and experimental works have been performed on the VFE-2 wing [8, 9, 10]. At the high angle of attack, another flow phenomenon called vortex breakdown appears on the wing in the trailing region. Luckring [11] has discussed very detailed effects of Reynolds number on the flow characteristics of the blunt-edged wing. In general, the development of primary vortex is delayed when the Reynolds number increased. This situation occurs because the stronger ability of turbulent boundary layer flow at the higher Reynolds number has slowed the separation process [12, 13]. The effect of leading-edge bluntness has been summarised by Luckring [14], and the leading-edge bluntness has influenced the onset and progression of the flow separation in the leading edge region.

In general, when the leading-edge bluntness increased, the development of primary vortex is delayed [15]. The flow characteristics above delta wing also changed when several active or passive flow control applied on the wing [16]. Active flow control is a technique that controls the vortical flow above delta wings which has various benefits, such as promoting or delaying flow separation, lift force enhancement, drag reduction, reduction of the wing and fin buffeting and suppress or enhance turbulence. Active and passive flow control techniques are used to modify vortex strength, location and structure [17, 18, 19, 20]. Current research carried out by Fahmi [21] has shown that the flow characteristics above the VFE-2 model can be controlled by a technique called 'blower'. During the experiment, Fahmi [21] has placed the blower at positions of 25% and 65% from the wing apex. However, this study could not confirm that this configuration has successfully brought the primary vortex to the apex of the wing. So, this project is carried out to observe the characteristic of primary vortex when the blower is placed in the apex region.

METHODOLOGY

In this project, the available UTM VFE-2 model has been used to investigate the effects of flow control on the wing. The design is based on the original geometry made by NASA [15]. The model has four sets of leading edges varying in their radii over the chord ratio of 0, 0.0005, 0.0015 and 0.0030 representing the sharp-edged, small-edged, medium-edged and large-edged wings. Figure 1 shows the engineering drawing of UTM VFE-2 delta wing model while the basic dimensions are shown in Table 1, and the model is made of aluminium.

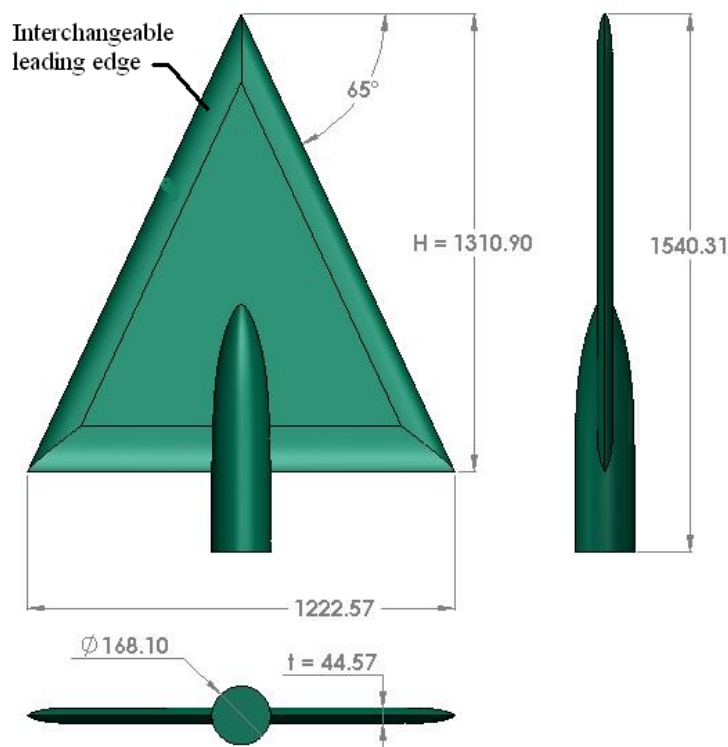
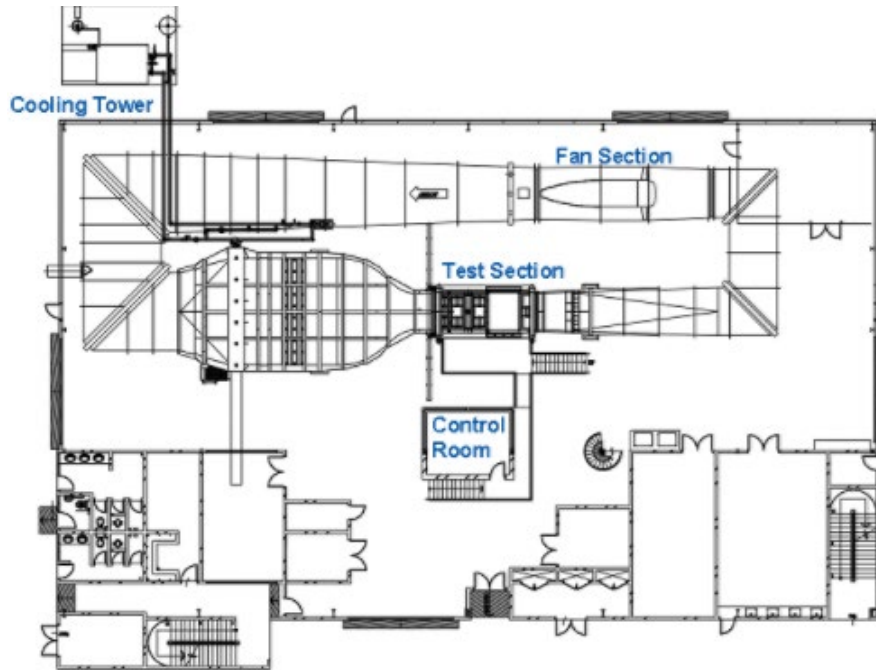


Figure 1. The geometry of UTM VFE-2 delta wing model.

Table 1. UTM VFE-2 delta wing model dimensions.

Description	Unit	Value
Root chord	m	1.311
Mean chord	m	0.612
Max span	m	0.611
Wing area	m ²	0.801
Sweep angle	degree	65°

The experiment was carried out in Universiti Teknologi Malaysia Low Speed Wind Tunnel (UTM-LST) with dimensions of 2.0m (width) \times 1.5m (height) \times 5.8m (length) with the maximum speed of 80 m/s. Figure 2 shows the layout of the UTM Wind Tunnel. During the experiments, two struts system were used to support the VFE-2 model in the test section. The trailing edge of the model is attached to a simple sting structure that can be adjusted manually to control the model angle of attack. One measurement technique was employed on the model, which was the surface pressure measurement. Figure 3(a) and 3(b) show the experimental set-up of VFE-2 at $\alpha=0^\circ$ and $\alpha=25^\circ$ in the test section of UTM Low Speed Wind Tunnel.

**Figure 2.** The layout of UTM-LST.

(a)



(b)

Figure 3. The model installation in UTM-LST at (a) $\alpha=0^\circ$ and (b) $\alpha=25^\circ$.

Test Configuration

The experiments were conducted at three different velocities of 9, 18 and 36 m/s that corresponding to 0.5×10^6 , 1.0×10^6 and 2.0×10^6 Reynolds numbers respectively. The model angles of attack were varying from $\alpha = 0^\circ$ to 25° . The

selection of Reynolds numbers was based on the work carried out by Tajuddin et al [10]. The experiments configuration is shown in Table 2. The blower momentum coefficient was then calculated based on Eq. (1) given [17].

$$C_{\mu} = m_j V_j / Q S_w \tag{1}$$

where C_{μ} indicates the blower momentum coefficient, m_j is the mass flow rate (1.22×10^{-4}), V_j is mean exit velocity of the blower (25 m/s), Q is dynamic pressure ($1/2 \rho v^2$) and S_w is delta wing surface area ($c^2 \times \tan \Lambda = 3.68 \text{ m}^2$).

Table 2. Test configuration.

Reynolds number	Velocity (m/s)	Angle of attack (°)	Blower coefficient, C_{μ}
0.5×10^6	9	0 - 25	1.74×10^{-5}
1.0×10^6	18	0 - 25	4.35×10^{-6}
2.0×10^6	36	0 - 25	1.08×10^{-6}

Pressure Distribution Method

The pressure distribution around the surface of the delta wing was measured using the pressure tubes installed inside the delta wing model, as shown in Figure 4. A digital pressure scanner with maximum of 30 ports was then connected to each of the tubes to measure the pressure. The pressure scanner is shown in Figure 5.

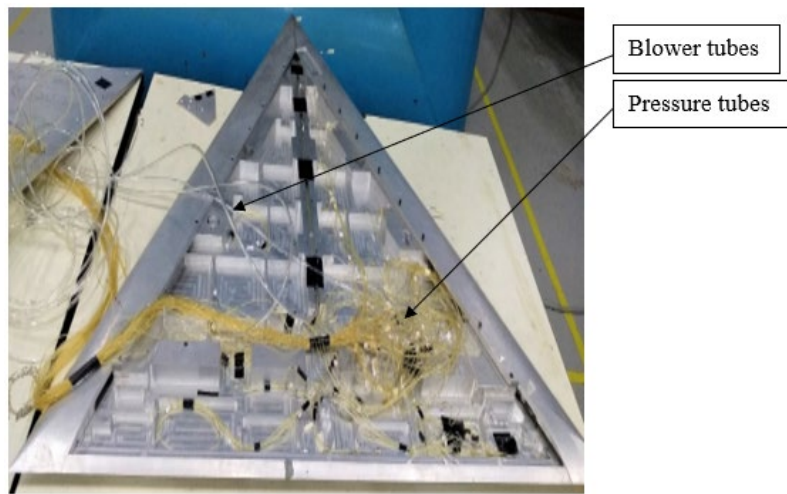


Figure 4. Installation of pressure tubes inside the wing.

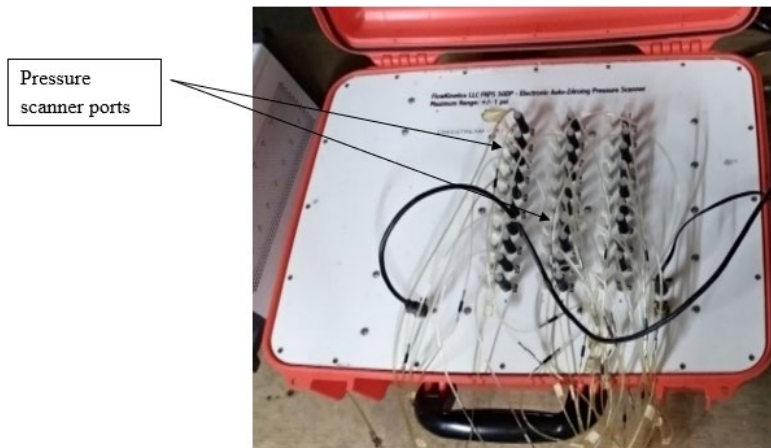


Figure 5. Pressure scanner.

Air Blower Experiment Setup

This section discusses the air blower technique carried out on UTM VFE-2 delta wing model. The blower tube with an inner diameter of 2.5 mm has been installed at three positions along the leading edge. The blower was placed at $Y/Cr = 0.05, 0.25$ and 0.65 from the leading edge, as shown in Figure 6. The high-speed air momentum is supplied by using air compressor located outside of the test section. In order to control the momentum of the air jet, a single channel hot wire was used to control the air blower at constant airspeed of 25 m/s. This is shown in Figure 7(a) and 7(b).

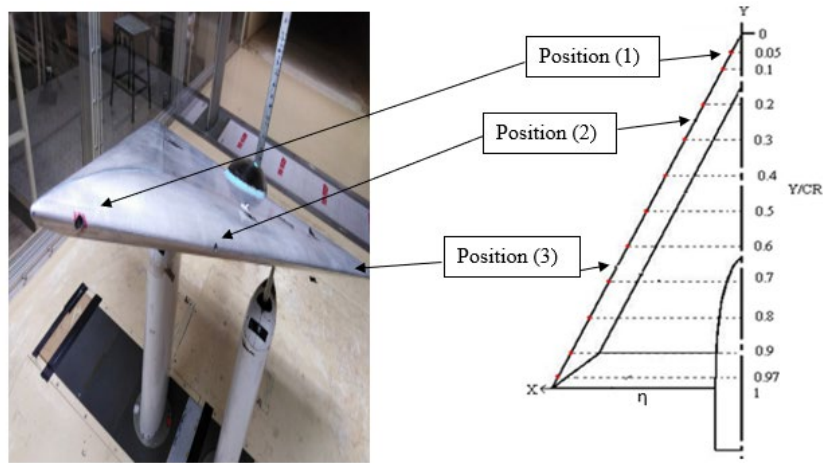


Figure 6. The blower positions along the leading edge.

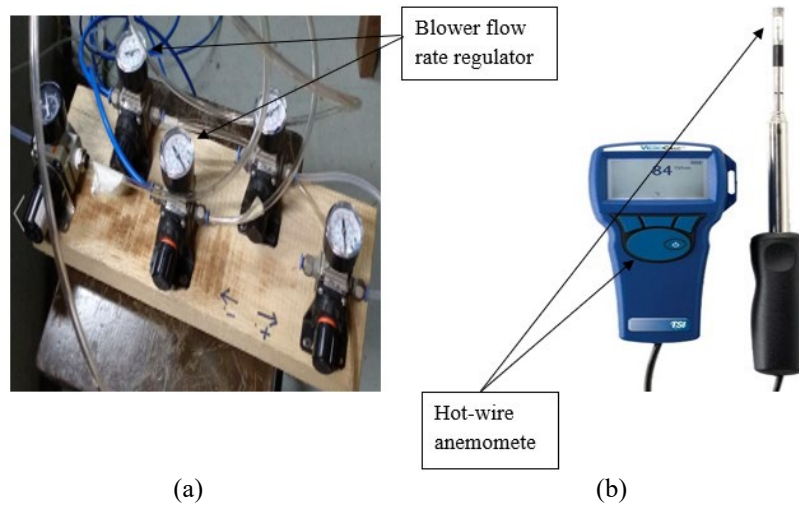


Figure 7. (a) Flow rate regulator and (b) hot-wire anemometer.

The experiments were carried out at Reynolds number of 0.5×10^6 , 1.0×10^6 and 2.0×10^6 and the angles of attack were varied at 0° , 10° , 13.3° , 18° , 23° and 25° . The experiments were conducted in 4 main phases. In the first phase, the experiment was conducted without the flow control technique; this experiment is called a clean wing experiment. The second phase experiment was conducted under the same flow conditions, but the blower was activated at position I (Y/CR at 0.05). The following experiments were the experiments when the blower is at position II (Y/CR at 0.25) and III (Y/CR at 0.65) were activated. For each set of the experiments, the surface pressure data were recorded at three times repeatability, and the sampling frequency was 0.01 Hz. The data obtained from the clean wing configuration was used to compare the effect of the blower at positions I, II and III.

Uncertainty Analysis

The pressure has been recorded at three times repeatability, and the sampling frequency was 0.01 Hz. The uncertainty analysis was also performed, and the standard error was then calculated for several selected points above the wing with a maximum uncertainty of about 0.7%.

RESULTS AND DISCUSSION

This section discusses the results obtained from the surface pressure measurement. In particular, the effects of angle of attack, Reynolds number, leading edge bluntness and blower will be discussed here. The onset of the primary vortex can be observed from the high suction peak near the leading edge. The primary vortex can be observed on the wing if there is a suction of pressure in the leading edge region.

Effect of Angle of Attack

The sampled results to unveil the effect of the angle of attack at constant Reynolds number of 0.5×10^6 are shown in Figure 8 below. The angles of attack were increased from 13.3° to 18° and 23° . At $\alpha = 13.3^\circ$, the primary vortex develops at about 30% from the wing apex. Upstream from this point, the flow is covered by the attached non-separated flow. When the angle of attack is $\alpha = 18^\circ$, the primary vortex is developed at about 30% from the wing apex. At the highest

angle of attack of $\alpha = 23^\circ$, the primary vortex has moved upstream to about 20% from the wing apex. This shows that the increase in the angle of attack has shifted the onset of the primary vortex further upstream. The results obtained from the present experiment are well agreed with Hummel [1] [8], Luckring [2] [4] and Mat et al [21].

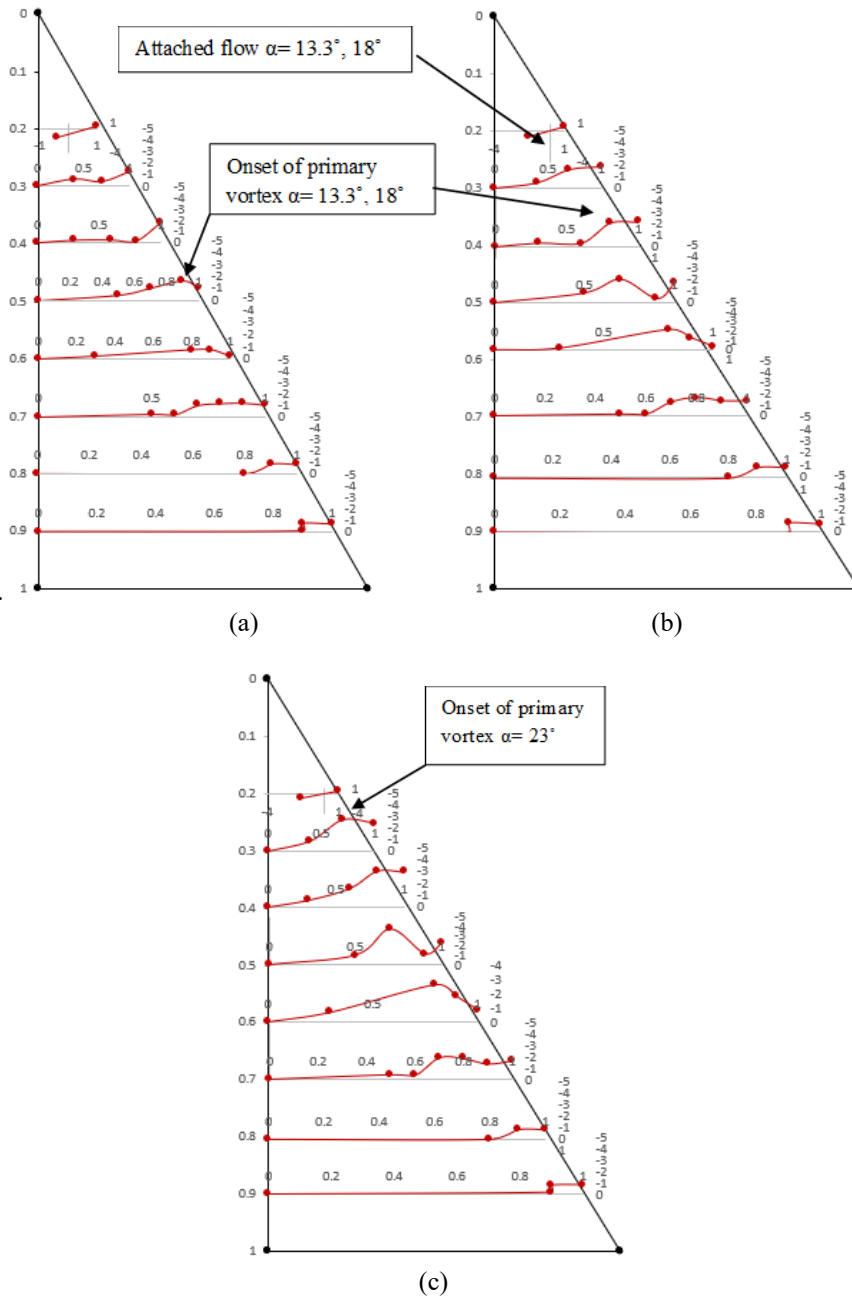


Figure 8. Effect of angle of attack on the onset of the primary vortex at (a) 0.5×10^6 , $\alpha = 13.3^\circ$, (b) 0.5×10^6 , $\alpha = 18^\circ$ and (c) 0.5×10^6 , $\alpha = 23^\circ$.

Effect of Reynolds Number

The effect of Reynolds number is done by comparing the data obtained at different Reynolds numbers of 0.5×10^6 , 1.0×10^6 and 2.0×10^6 at a constant angle of attack and leading-edge bluntness, as shown in Figure 9. For this case, the comparison was made on the medium-edged wing at an angle of attack of 13.3° . From the figure, the onset of the primary vortex developed at about 50% from the wing apex when the Reynolds number is 0.5×10^6 and at about 60% from the wing Apex when the Reynolds number is 1.0×10^6 . It is interesting to notice that the primary vortex developed at about 70% from the wing Apex when the Reynolds number increased to 2.0×10^6 . The result here has shown that the Reynolds number has delayed the development of the primary vortex. The results consist with Hummel [1] [8], Luckring [2] [4], Said [12] [13] and Mat et al [21].

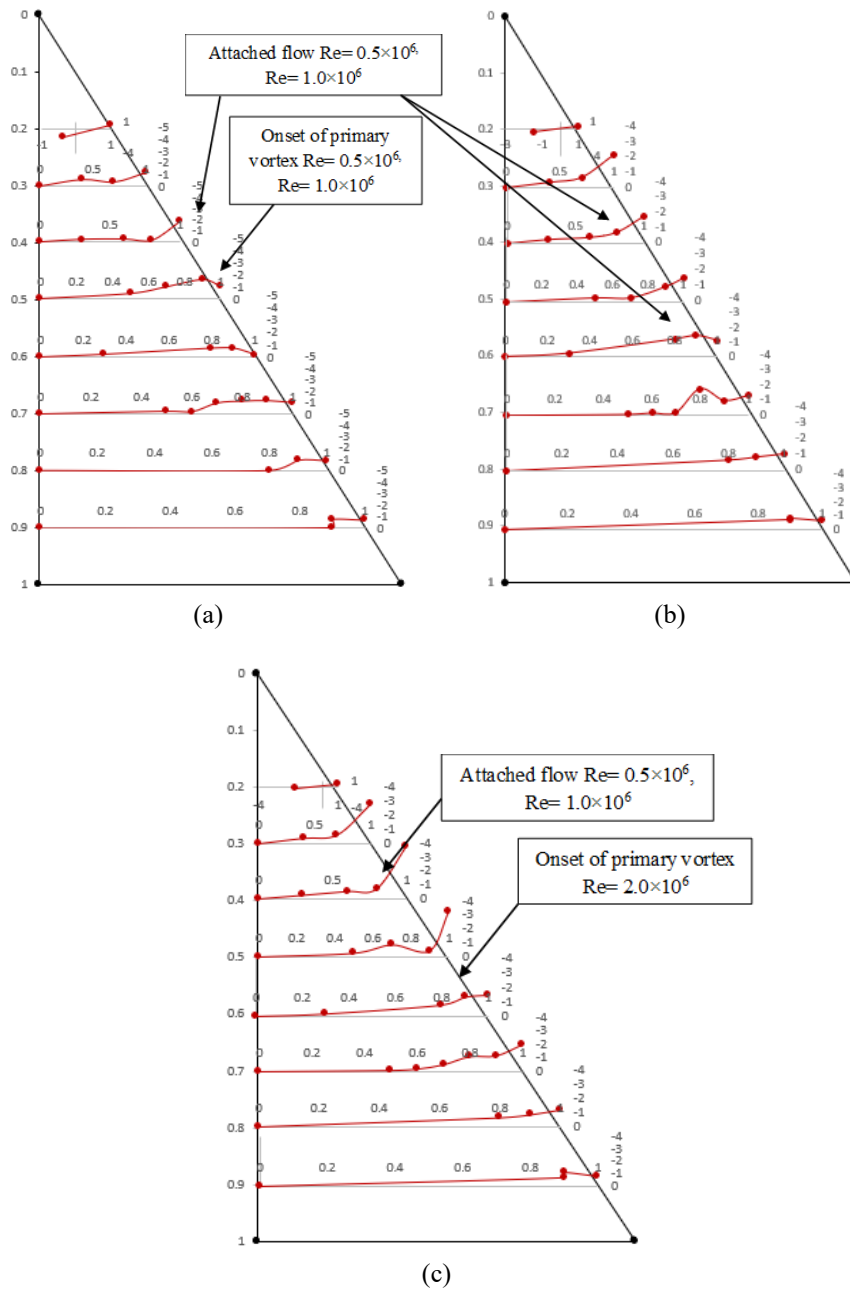


Figure 9. Influence of Reynolds number on the flow topology at Reynolds number of (a) 0.5×10^6 , (b) 1.0×10^6 and (c) 2.0×10^6 at the angle of attack of 13.3° .

Effect of Leading-Edge Bluntness

The sampled data to compare the effect of leading-edge bluntness is shown in Figure 10. In this case, the data obtained from the medium-edge model at a Reynolds number of 0.5×10^6 and $\alpha = 13.3^\circ$ is shown. The result has shown that the attached flow covered around 30% of the wing from the apex. The primary vortex is observed at 40% from the wing apex.

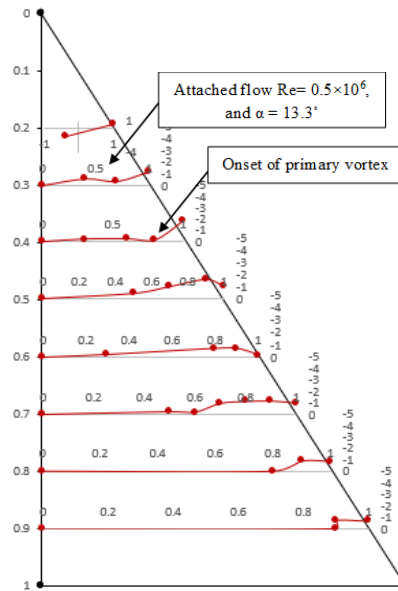
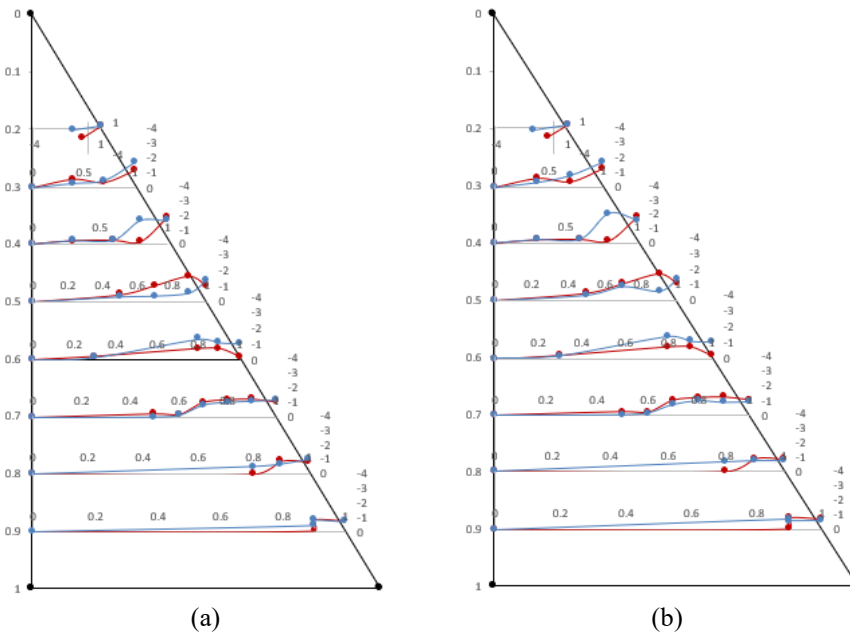
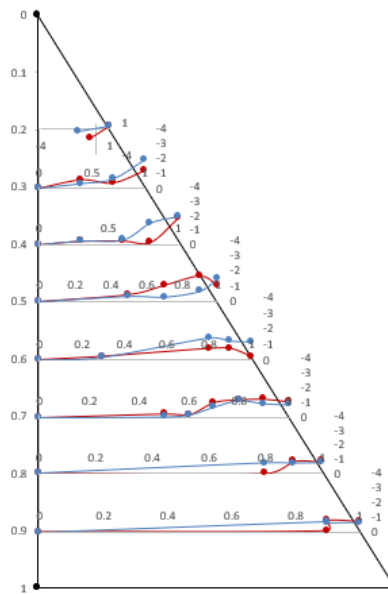


Figure 10. Effect of leading-edge bluntness at $Re= 0.5 \times 10^6$ and $\alpha= 13.3^\circ$.

Effect of Air Blower on the Flow Topology

This section discusses the effect on the flow topology when the air jet at 25 m/s flow control (blower) is applied at three different positions, namely, blower I, II and III. For all cases, the data obtained from the clean wing configuration (red plot) is compared with those from the blower effects (blue plot). The comparison at low Reynolds number of 0.5×10^6 is shown in Figure 11. When the flow control is positioned as Blower I, shown in Figure 11(a), a very obvious effect is noticed at $Y/Cr = 0.4$. At this point, the flow control has initiated the development of the primary vortex compared to clean wing configuration. Upstream from this position, the flow is still attached to the wing surface. A similar situation happened when the flow control is positioned as Blower II in Figure 11(b). It shows that the flow control has initiated the flow separation earlier compared to the clean wing configuration. A similar situation happened when the flow control is located as Blower III in Figure 11(c); it shows that the flow control can initiate earlier separation process.

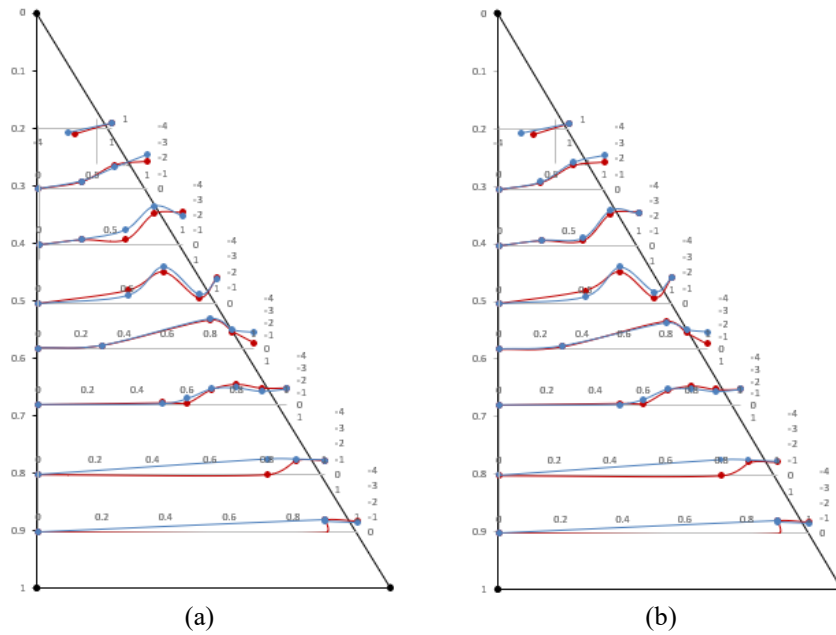




(c)

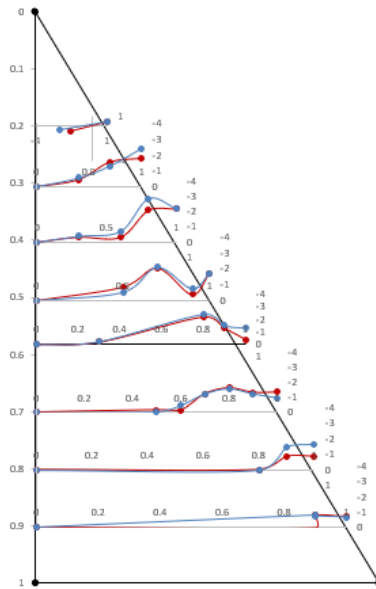
Figure 11. Effect of the blower at $Re = 0.5 \times 10^6$, $\alpha = 13.3^\circ$ for (a) blower 1, (b) blower 2 and (c) blower 3.

The effects of flow control when the angle of attack is increased to $\alpha = 18^\circ$ at Reynolds number of 0.5×10^6 are shown in Figure 12. There is a remarkable feature of the flow topology under this flow condition, for both cases of Blower I and II, it can be observed here that the primary vortex has formed at the same position. However, the flow control at both positions has increased the size of the primary vortex significantly. This can be observed with the suction peak for the blue-lined is relatively bigger when compared to the red-lined suction peak.



(a)

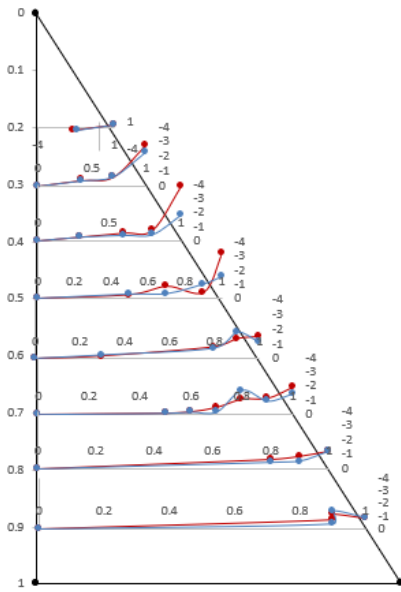
(b)



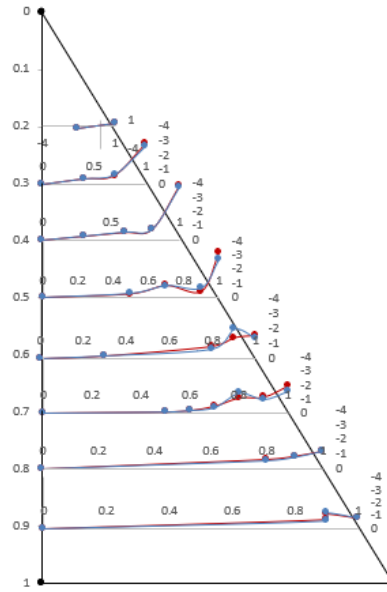
(c)

Figure 12. Effect of the blower at $Re = 0.5 \times 10^6$, $\alpha = 18^\circ$ (a) blower 1, (b) blower 2 and (c) blower 3.

The effect due to the blower at a higher Reynolds number of 2×10^6 is shown in Figure 13. For this case, no significant difference noted as far as the effect of flow control on the flow topology is concerned. As noted, the lines of the primary vortex for without flow control and with flow control have shown identical to each other. This condition may be linked with the stronger ability of turbulent boundary layer to delay the flow separation. This is also because the air jet produced by the blower (25 m/s) is lower than the tunnel speed to get the Reynolds number of 2×10^6 (36 m/s).



(a)



(b)

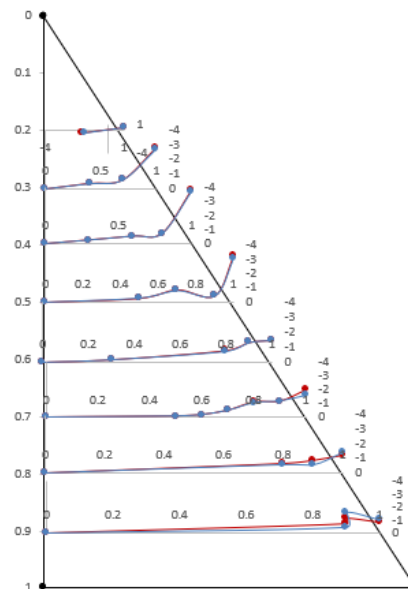


Figure 13. Effect of the blower at $Re= 2.0 \times 10^6$, $\alpha= 13.3^\circ$ for (a) blower 1, (b) blower 2 and (c) blower 3.

CONCLUSION

A very detailed study has been carried out to investigate the effects of angle of attack, Reynolds number, leading-edge bluntness on the flow characteristics of blunt-edged delta wing VFE-2 configuration. The increase in the angle of attack has accelerated the formation of the primary vortex while the increase in Reynolds number and leading-edge bluntness have an opposite effect. The effect of flow control, called 'blower', has been studied in detail. It can be observed that the position of flow control affecting the formation of the primary vortex. At low Reynolds number of 0.5×10^6 , the flow control has accelerated the process of primary vortex development. When the Reynolds number increased to 1×10^6 , the flow control has increased the size of the primary vortex significantly. When the Reynolds number is 2×10^6 , no effect occurs; this is because the jet momentum generated by the blower is lower than the speed of testing. Another main observation from this experiment is that even the flow control is placed in the apex region, the attached flow still exists. More experiments with stronger air jet from the blower could be done in the future.

ACKNOWLEDGEMENT

This research was funded by the grants from Universiti Teknologi Malaysia (21H05, 18H06 and 4Y225). The experiments have been carried out in Universiti Teknologi Malaysia Aerolab. The data presented, the statement made and views expressed are solely the responsibility of the authors.

REFERENCES

- [1] Hummel DJ. The international vortex flow experiment 2 (VFE-2): Background, objectives and organization. *Aerospace Science and Technology* 2013; 24(1): 1-9.
- [2] Luckring JM. Chapter 4- Experimental investigation of the flow about a 65° delta wing in the NASA Langley national transonic facility. Report for NATO Science and Technology Organization. Report no. RTO-TR-AVT-080, 6 October 2009. RTO.
- [3] Gad-el-Hak M, Blackwelder RF. The discrete vortices from a delta wing. *American Institute of Aeronautics and Astronautics Journal* 1985; 23(6): 961-2.
- [4] Luckring JM, Boelens OJ. A unit-problem investigation of blunt leading-edge separation motivated by AVT-161 SACCON research. Report for NATO Science and Technology Organization. Report no. RTO-MP-AVT-189, 12 October 2011.
- [5] Hummel D. On the vortex formation over a slender wing at large angles of incidence. *AGARD Conference Proceedings* 1979; 247: 15-1-15-17.
- [6] Konrath R, Klein C, Schröder A. PSP and PIV investigations on the VFE-2 configuration in sub-and transonic flow. *Aerospace Science and Technology* 2013; 24(1): 22-31.
- [7] Fritz W, Cummings RM. Chapter 34- Lessons learned from the numerical investigations on the VFE-2 configuration. In: *Understanding and Modeling Vortical Flows to Improve the Technology Readiness Level for Military Aircraft*. Report for NATO Science and Technology Organization. Report no. RTO-TR-AVT-113, 28 October 2009.
- [8] Luckring JM, Hummel D. Chapter 24- What was learned from the new VFE-2 experiments? In: *46th AIAA Aerospace Sciences Meeting and Exhibit*, Reno, Nevada, USA; 7-10 January, 2008.
- [9] Tajuddin N, Mat S, Said M, Mansor S. Flow characteristic of blunt-edged delta wing at high angle of attack. *Journal of Advanced Research in Fluid Mechanics and Thermal Sciences* 2017; 39(1): 17-25.
- [10] Schütte A. Numerical investigations of vortical flow on swept wings with round leading edges. *Journal of Aircraft* 2017; 54(2): 572-601.

- [11] Luckring J. Reynolds number and leading-edge bluntness effects on a 65-deg delta wing. In: 40th AIAA Aerospace Sciences Meeting and Exhibit, Reno, Nevada, USA; 14-17 January 2002.
- [12] Said M, Mat S. Effects of Reynolds number on the onset of leading-edge vortex separation above blunt-edge delta wing VFE-2 configurations. In: 30th Congress of the International Council of the Aeronautical Sciences, Daejeon, South Korea, pp. 25-30; 2016.
- [13] Said M, Mat SB, Mansor S, Abdul-Latif A, Mat Lazim T. Reynolds Number effects on flow topology above blunt-edged delta wing VFE-2 configurations. In: 53rd AIAA Aerospace Sciences Meeting, Kissimmee, Florida, USA, pp. 1229; 2015.
- [14] Luckring JM. Initial experiments and analysis of blunt-edge vortex flows for VFE-2 configurations at NASA Langley, USA. *Aerospace Science and Technology* 2013; 24(1): 10-21.
- [15] Said M, Mat S, Mansor S, Ali A. Effects of leading-edge enlargement on the primary vortex of blunt-edged delta wing VFE-2 profile. *Acta Polytechnica Hungarica* 2018; 15(8): 7-28.
- [16] Gursul I, Wang Z, Vardaki E. Review of flow control mechanisms of leading-edge vortices. *Progress in Aerospace Sciences* 2007; 43(7-8): 246-70.
- [17] Renac F, Barberis D, Molton P. Control of vortical flow over a rounded leading-edge delta wing. *American Institute of Aeronautics and Astronautics Journal* 2005; 43(7): 1409-18.
- [18] Okada S, Muramatsu S, Hiraoka K. Control of the vortex breakdown on a delta wing by blowing. In: 24th International Congress of The Aeronautical Sciences, Yokohama, Japan, pp. 1-8; 2004.
- [19] Mitchell A, Morton S, Molton P, Guy Y. Flow control of vortical structures and vortex breakdown over slender delta wings. In: RTO AVT Symposium on Advanced Flow Management: Part A – Vortex Flows and High Angle of Attack for Military Vehicles, Loen, Norway; 7-11 May 2001.
- [20] Rein M, Busse F, Edzards F, Haselmeyer H, Höhler G, Siegel L. Flow control of non-slender delta wings by leading-edge modifications. *Fluid Dynamics Research* 2020; 52(1): 015517.
- [21] Mat SB, Abdullah MF, Dahalan MN, Said MB, Mansor S, Abdul-Latif A, Mat Lazim T. Effects of Synthetic Jet Actuator (SJA) on flow topology of blunt-edged UTM VFE2 wing model. In: 55th AIAA Aerospace Sciences Meeting 2017, Texas, USA. pp. 0326.